Short-range ordering in face-centered-cubic Ni_3Al

J. K. Okamoto, C. C. Ahn, and B. Fultz
Division of Engineering and Applied Science, 138-78, California Institute of Technology, Pasadena, California 91125

(Received 25 March 1994; accepted for publication 9 January 1995)

Films of fcc Ni_3Al with suppressed short-range order (SRO) were prepared by physical vapor deposition of Ni_3Al onto room-temperature substrates. Extended electron energy-loss fine-structure spectra were obtained from both Al K and Ni L_{23} edges. After the samples were annealed for various times at 150 °C, a moderate growth of SRO was observed in the first-nearest-neighbor environments of both the Al and Ni atoms. As prepared, these fcc Ni_3Al materials, and presumably others having similar heat evolutions as measured by differential scanning calorimetry, have a high degree of chemical disorder. © *1995 American Institute of Physics.*

I. INTRODUCTION

Recently several groups have synthesized chemically disordered face-centered cubic (fcc) Ni_3Al by ball milling[1–3] laser quenching,[4] and physical vapor deposition.[5] These materials were unstable against $L1_2$ ordering, which developed upon annealing at temperatures of 300 °C and above. The reported heat evolutions in differential scanning calorimetry (DSC) traces were very similar,[1–3,5] having an early exothermic peak near 150 °C, and a larger exothermic peak starting near 300 °C. In all cases, x-ray diffractometry showed that the larger peak is associated with both long-range ordering (LRO) and grain growth. The origin of the exothermic peak at 150 °C is less obvious, however. Baró *et al.*[2] suggested that it originated with defect recovery, but Harris *et al.*[5] suggested that it originated with the onset of short-range ordering (SRO). Here we report extended electron energy-loss fine-structure
(EXELFS) measurements on the chemical short-range order in the first-nearest-neighbor (1nn) shells of both Al and Ni atoms.

II. EXPERIMENT

We used an ingot of Ni_3Al that was prepared previously.[5] A 5 mg piece was evaporated in a resistively heated tungsten basket in a Denton DV-502 thermal evaporator evacuated to approximately 1×10^{-6} Torr. Thin-film samples of approximately 100 nm thickness were deposited on rock salt substrates placed about 2.3 cm above the tungsten basket.[6] Samples for EXELFS were prepared by floating the films from the rock salt in distilled water, and collecting pieces on copper transmission electron microscopy grids.

Electron energy-loss spectra were acquired with a Gatan 666 parallel detection magnetic prism spectrometer attached to a Phillips EM 430 transmission electron microscope. The energy resolution at the detector was about 7 eV with a dispersion of 2.1 eV per channel. The spectra were obtained at a temperature of 97 K using a collection angle of 8 mrad. To minimize electron-beam heating, the spectra were collected from regions 20 μm in diameter with 200 keV electrons and a beam current of 50 nA. Gain fluctuations in the detector system were removed by a two-step process described by Shuman and Kruit.[7] Each spectrum was first divided by a gain-calibration spectrum obtained in the "uniform illumination mode" of the Gatan 666. Next, gain averaging was performed over 20 individual spectra, each shifted by about three detector elements. The averaged data contained several million counts per channel near the absorption edges. For thin samples the oscillating intensity in the extended region should not be sensitive to plural scattering,[8] so the spectra were not deconvoluted. The smoothly varying parts of the energy-loss data were fit to cubic spline polynomials with knots spaced approximately evenly in k space. The EXELFS oscillations χ were normalized to the heights of the edge jumps, and calculated differential cross sections were used to correct for the basic nonoscillatory edge shapes.

III. EXELFS DATA ANALYSIS

The simple structure of the Al K edge allowed a straightforward analysis of the Al K-edge EXELFS, and our procedure was described previously.[9,10] Analysis of the Ni L-edge EXELFS is less straightforward, owing to the variety of possible initial and final angular momentum states of L-edge transitions. Leapman *et al.*[11] demonstrated the feasibility of obtaining useful EXELFS data from L_{23} edges of the $3d$ transition-metal elements. One of the authors has considered this problem in detail,[8,10] and a few important considerations are mentioned here. The spin-orbit splitting of 17 eV between Ni L_3 and L_2 edges can be neglected in the analysis because at energies far above the ionization threshold of 854 eV, the EXELFS oscillations from L_3 and L_2 edges will be nearly in phase. The presence of the Ni L_1 edge which appears 153 eV beyond the L_3 threshold complicates the analysis of Ni L_{23} EXELFS for two reasons. First, the L_1-edge jump overlaps with the L_{23} EXELFS signal as shown in Fig. 1. This problem is avoided by using only L_{23} EXELFS data sufficiently past the L_1-edge jump. Second, the L_1 EXELFS overlaps with the L_{23} EXELFS.

An estimate of the importance of this second effect from the L_1 EXELFS overlap required calculations of differential electron-scattering cross sections.[12] Atomic Hartree–Slater wave functions from the algorithm of Herman and Skillman[13] were used as the initial states while the final states were continuum states with a free-electron density of states.[14] The calculations used a collection angle of 8 mrad which corresponds to our experimental conditions, and our calculations ignored spin-orbit splitting. In the region of in-

 0021-8979/95/77(9)/4380/4/$6.00

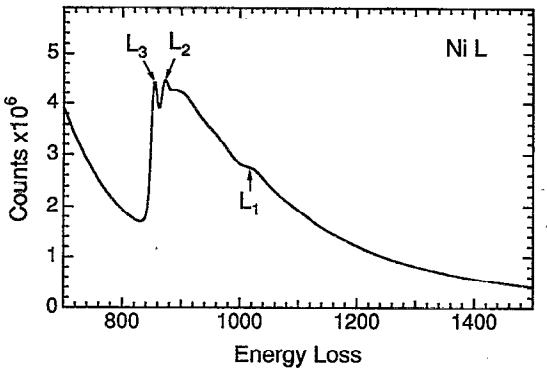

FIG. 1. Ni L-edge data from ordered Ni_3Al after gain averaging showing overlap of transitions to continuum states. Transitions to bound L_3 and L_2 states occur at 854 and 871 eV while the smaller L_1 edge begins at 1008 eV.

terest, the differential cross section of the Ni L_1 edge was about 4× smaller than that of the Ni L_{23} edge. Moreover, transforming the L_1 EXELFS oscillations from energy-loss space to the k space corresponding to the L_{23} edge raises the frequencies of the L_1 EXELFS oscillations, making them incoherent.

We also considered the effects of different final states after transitions from the $2p$ core states. Calculations of differential scattering cross sections were performed for the excitation of Ni $2p$ electrons into final states of s, p, d, or f character. It was found that in the EXELFS region, the electric dipole-allowed $2p$ to d transition dominates over the sum of all others by a factor of over 20. This dominance of the $2p$ to d transition makes possible the interpretation of the 1nn shell Ni L_{23} EXELFS using a form of the standard plane-wave EXAFS equation[15]

$$\chi(k)=(-1)^{l_0+1}\sum_j \frac{|f_j(\pi,k)|S_j(k)}{kR_j^2}\, e^{-2R_j/\lambda(k)}e^{-2\sigma_j^2k^2} \times\sin[2kR_j+\eta_j(\pi,k)+2\delta_{l_0+1}(k)], \quad (1)$$

for angular momentum quantum number l_0, distance from central to neighboring atom R_j for atom j, and amplitude and phase shifts $|f_j(\pi,k)|$ and $|\eta_j(\pi,k)|$ respectively, for polycrystalline samples with outgoing d waves.

Using *ab initio* plane-wave calculations of amplitude and phase functions for EXAFS from Teo and Lee,[15] we calculated the theoretical contribution to the EXELFS from the 1nn shell for various states of SRO in the 1nn shell of Ni_3Al. These computations were made by Fourier band-pass filtering of $k^2\chi(k)$ determined from Eq. (1) using

$$F(k^n\chi)=\int_{k_{\min}}^{k_{\max}} W(k)k^2\chi(k)\cos(2kR)dk + i\int_{k_{\min}}^{k_{\max}} W(k)k^2\chi(k)\sin(2kR)dk, \quad (2)$$

where $W(k)$ is a window function whose edges are smoothed by Gaussian line shapes to reduce ringing, and by taking the Fourier-transform magnitude $|F(k^2\chi)|$.

Figure 2 compares the theoretical 1nn peaks from a random fcc solid solution of Ni_3Al with that from an ordered

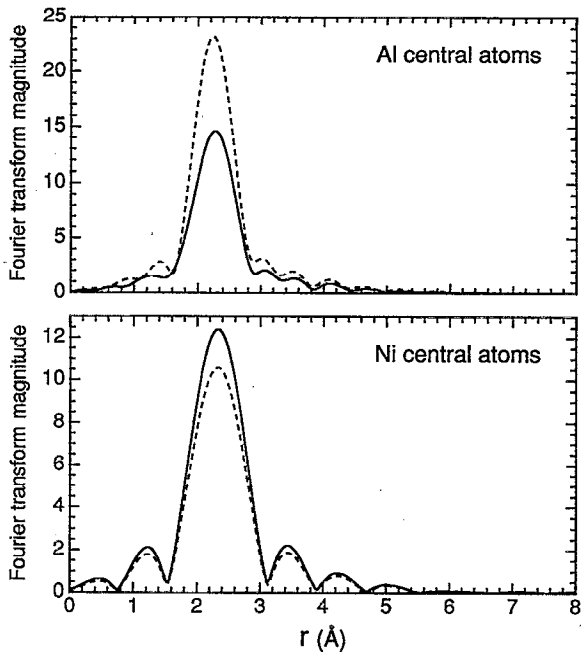

FIG. 2. Fourier transforms of *ab initio* calculations of Al K EXELFS ($4<k<10$ Å^{-1}) and Ni L_{23} EXELFS ($8.5<k<12.5$ Å^{-1}) from 1nn shell in Ni_3Al. Calculations presented for both fully disordered (solid line) and ordered (dashed line) alloys. 1nn shell distance of 2.52 Å is assumed but no phase-shift correction has been applied. EXELFS weighted by k^2 before Fourier transformation.

alloy with $\alpha(1)=-0.333$ (this corresponds to perfect $L1_2$ or $D0_{22}$ order, for example). The theoretical changes in the heights of the 1nn peaks for the Al and Ni EXELFS, H_1^{Al} and H_1^{Ni}, were calculated from Eq. (1) as functions of the Warren–Cowley SRO parameter $\alpha(1)$.[16] The fractional changes in the heights of these 1nn peaks with respect to a disordered solid solution are

$$\frac{dH_1^{\mathrm{Al}}}{d\alpha(1)}=-1.68, \quad (3)$$

$$\frac{dH_1^{\mathrm{Ni}}}{d\alpha(1)}=+0.45. \quad (4)$$

As $\alpha(1)$ becomes negative, the height of the 1nn peak should increase for Al central atoms, but should decrease for Ni central atoms. This is reasonable, since the backscattering depends strongly on the changes in the number of 1nn Ni atoms.

IV. RESULTS AND DISCUSSION

Figure 3 shows the experimental Al K and Ni L_{23} EXELFS oscillations χ from the as-evaporated Ni_3Al sample. Figure 4 presents Fourier transforms of the EXELFS from the as-evaporated sample and from the same region of the same sample after annealing at 150 °C for 210 min. The peaks near 1 Å are artifacts from residual low-frequency oscillations of the spline fits. The positions of the experimental 1nn peaks are in good agreement with the calculated positions shown in Fig. 1. Figure 5 presents the changes in heights of the experimental 1nn peaks as functions of anneal-

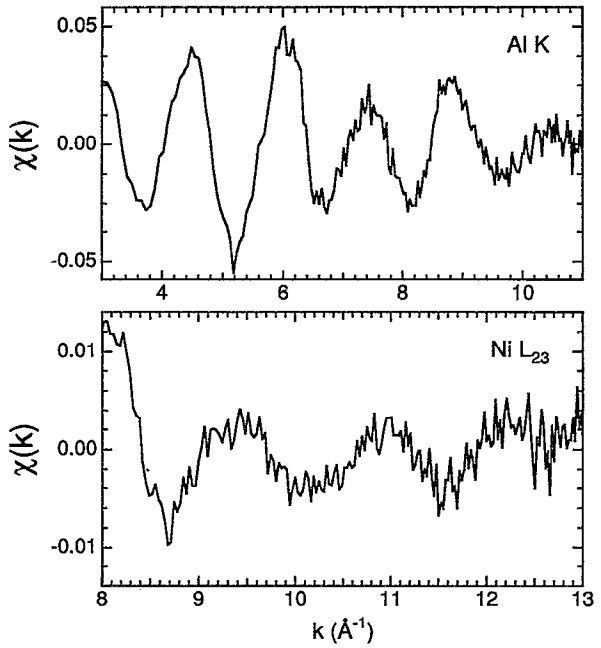

FIG. 3. Unweighted EXELFS oscillations χ from Al K and Ni L_{23} edges in as-evaporated Ni_3Al samples. Data taken with sample at 97 K.

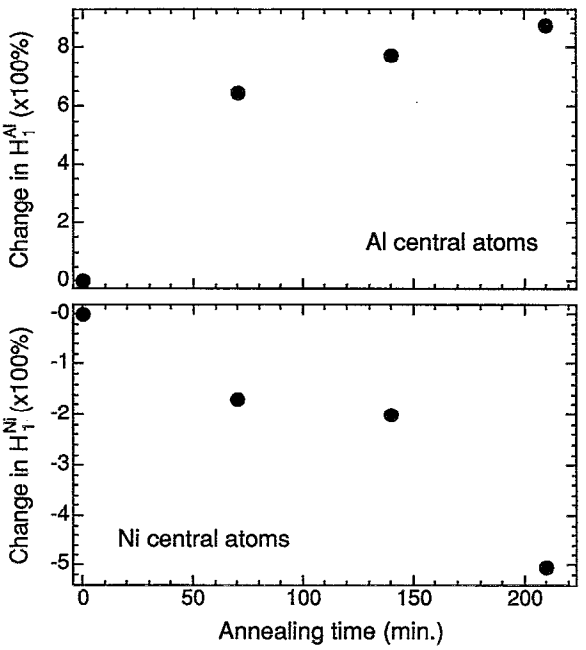

FIG. 5. Experimental changes in heights of 1nn peaks as function of annealing time at 150 °C. Percent change with respect to height of 1nn peak in as-evaporated sample.

ing time. The data show an increase in SRO as the Ni_3Al sample is annealed at 150 °C. As expected from the *ab initio* calculations of short-range ordering, increases in the height of the 1nn peak for Al central atoms are accompanied by smaller decreases in the height of the 1nn peak for Ni central atoms.

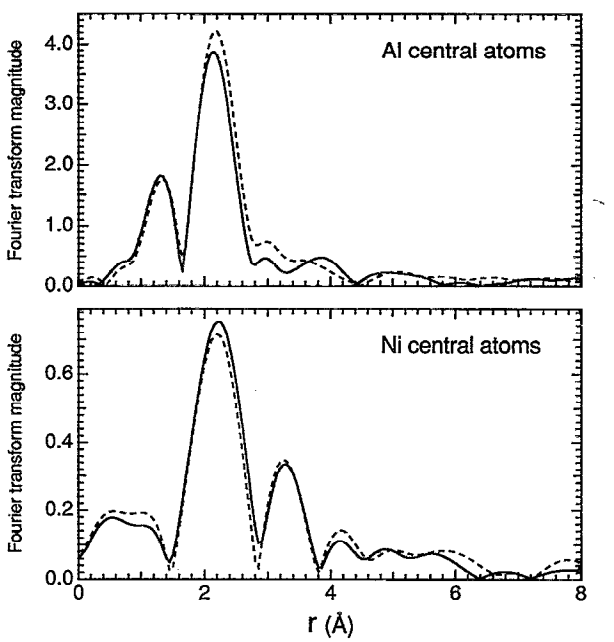

FIG. 4. Fourier transforms of experimental Al K EXELFS ($4<k<10$ Å^{-1}) and Ni L_{23} EXELFS ($8.5<k<12.5$ Å^{-1}) in Ni_3Al. Experimental data presented from sample both as evaporated and after annealing at 150 °C for 210 min. Data taken at 97 K. No phase-shift correction has been applied.

By interpreting the data of Fig. 5 with Eqs. (3) and (4), we find that after 210 min of annealing at 150 °C, the change in the Warren–Cowley SRO parameter $\alpha(1)$ is approximately -0.08 ± 0.02. This is a large change, since $\alpha(1)$ can change only from 0.0 in a disordered solid solution to -0.33 for perfect $L1_2$ order. No LRO was observed in the electron-diffraction patterns from this annealed material, and this temperature is well below the previously reported temperatures for long-range ordering.[1–5] Although it is unlikely that the as-evaporated material is a fully random solid solution, this increase in SRO upon annealing indicates that the as-evaporated material is rather disordered on the 1nn length scale.

Such a change in SRO could well account for the exothermic peak between 150 and 250 °C in DSC traces. If the enthalpy of ordering were proportional to the change in $\alpha(1)$, the observed change in SRO would account for one-quarter of the ordering enthalpy, or about 2 kJ/mol.[5] The similar enthalpy release at 150 °C from fcc Ni_3Al materials prepared by ball milling[1–3] indicates that these materials also possess significant short-range disorder.

While our EXELFS data prove that SRO is evolving in fcc Ni_3Al annealed at 150 °C, these data do not prove that the type of order is $L1_2$. In particular, the formation of $L1_0$ order will give similar results, and perhaps the many variants of $L1_0$ order may allow it to form transiently, much as a transient $B32$ order forms in Fe_3Al.[17] The independent peaks observed in the DSC traces suggest that the short-range ordering at 150 °C is a different process than the long-range $L1_2$ ordering that occurs at 300 °C.

V. CONCLUSION

In summary, EXELFS data from both the Al K and Ni L_{23} edges were used to measure the changes in chemical short-range order in Ni_3Al. SRO was found to develop upon annealing at 150 °C, corresponding to a change in SRO parameter $\alpha(1)$ of about -0.08 ± 0.02. This moderate evolution of SRO before the onset of $L1_2$ LRO shows that the as-evaporated fcc Ni_3Al is substantially short-range disordered. The early onset of SRO seems consistent with a heat release that has been reported previously in the temperature range of 100–250 °C.

ACKNOWLEDGMENTS

We thank Dr. P. Rez for providing the software used to calculate the electron-scattering cross sections, and Dr. D. H. Pearson for his help with the calculations. This research was supported by the U. S. Dept. of Energy under Contract No. DE-FG03-86ER45270.

[1] J. S. C. Jang and C. C. Koch, J. Mater. Res. **5**, 498 (1990).
[2] M. D. Baró, J. Malagelada, S. Suriñach, N. Clavaguera, and M. T. Clavaguera-Mora, in *Ordering and Disordering in Alloys*, edited by A. R. Yavari (Elsevier, Essex, 1992), p. 55.
[3] A. R. Yavari, P. Crespo, E. Pulido, A. Hernando, G. Fillion, P. Lethuiller, M. D. Baró, and S. Suriñach, in *Ordering and Disordering in Alloys*, edited by A. R. Yavari (Elsevier, Essex, 1992), p. 12.
[4] J. A. West, J. T. Manos, and M. J. Aziz, Mater. Res. Soc. Symp. Proc. **213**, 859 (1991).
[5] S. R. Harris, D. H. Pearson, C. M. Garland, and B. Fultz, J. Mater. Res. **6**, 2019 (1991).
[6] By analyzing a spectrum of the low-loss region, the sample thickness was found to be 0.5×the mean free path of inelastic scattering.
[7] H. Shuman and P. Kruit, Rev. Sci. Instrum. **56**, 231 (1985).
[8] J. Kozo Okamoto, Ph.D. dissertation in Applied Physics, California Institute of Technology, May 6, 1993.
[9] J. K. Okamoto, C. C. Ahn, and B. Fultz, *Microbeam Analysis—1990*, edited by J. R. Michael and P. Ingram (San Francisco Press, San Francisco, 1990), p. 56.
[10] J. Okamoto, D. H. Pearson, C. C. Ahn, and B. Fultz, in *Transmission Electron Energy Loss Spectrometry in Materials Science*, edited by M. Disko, C. C. Ahn, and B. Fultz (RMS, Warrendale, 1992), p. 183.
[11] R. D. Leapman, L. A. Grunes, and P. L. Fejes, Phys. Rev. B **26**, 614 (1982).
[12] H. A. Bethe, Ann. Phys. **5**, 325 (1930).
[13] F. Herman and S. Skillman, *Atomic Structure Calculations* (Prentice-Hall, Englewood Cliffs, NJ, 1963).
[14] R. D. Leapman, P. Rez, and D. F. Mayers, J. Chem. Phys. **72**, 1232 (1980).
[15] B. K. Teo and P. A. Lee, J. Am. Chem. Soc. **101**, 2815 (1979). Software implemented by R. A. Scott.
[16] B. E. Warren, *X-Ray Diffraction* (Addison-Wesley, Reading, MA, 1969), p. 229.
[17] Z. Q. Gao and B. Fultz, Philos. Mag. B **67**, 787 (1993).